Field observation of wave damping by fluid mud

Meirelles Nunes Da Rocha, S.; Vinzon, Susana B.

DOI
10.1016/j.margeo.2016.03.006

Publication date
2016

Document Version
Accepted author manuscript

Published in
Marine Geology

Citation (APA)
Meirelles Nunes Da Rocha, S., & Vinzon, S. B. (2016). Field observation of wave damping by fluid mud. *Marine Geology*, *376*, 194-201. https://doi.org/10.1016/j.margeo.2016.03.006

Field observation of wave damping by fluid mud

Article *in* Marine Geology · March 2016

DOI: 10.1016/j.margeo.2016.03.006

2 authors:

Saulo Meirelles
Delft University of Technology

Susana B. Vinzon
Federal University of Rio de Janeiro

Accepted Manuscript

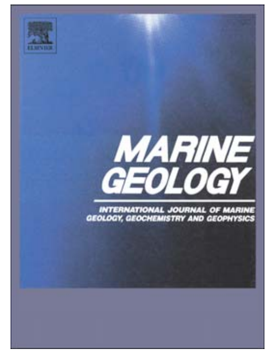

Field observation of wave damping by fluid mud

Saulo Meirelles, Susana B. Vinzon

PII: S0025-3227(16)30022-6
DOI: doi: 10.1016/j.margeo.2016.03.006
Reference: MARGO 5426

To appear in: *Marine Geology*

Received date: 13 September 2015
Revised date: 16 February 2016
Accepted date: 8 March 2016

Please cite this article as: Meirelles, Saulo, Vinzon, Susana B., Field observation of wave damping by fluid mud, *Marine Geology* (2016), doi: 10.1016/j.margeo.2016.03.006

Marine Geology xxx (2015) xxx–xxx

Contents lists available at ScienceDirect

Marine Geology

journal homepage: www.elsevier.com/locate/margo

Letter

Field observation of wave damping by fluid mud

Saulo Meirelles [a,*,1], Susana B. Vinzon [b]

[a] Hydraulic Engineering Department, Delft University of Technology, Stevinweg 1, 2628CN Delft, the Netherlands
[b] Department of Coastal & Oceanographic Engineering, Federal University of Rio de Janeiro, Rio de Janeiro, Brazil

ARTICLE INFO

Article history:
Received 13 September 2015
Received in revised form 16 February 2016
Accepted 8 March 2016
Available online xxxx

Keywords:
Wave–mud interaction
Viscous dissipation
Cassino Beach

ABSTRACT

Extensive mud deposits are found off Cassino Beach, Brazil. The wave damping over the muddy bottom was studied using field measurements. By applying a technique of spectral analysis we showed that the wave attenuation occurred differently throughout the wave spectra. Field measurements revealed that the maximum wave energy dissipation took place over the deposit's depocenter and that lutocline height varied significantly in the order of days. The results indicated that short waves (from 3.75 to 6.25 s) underwent the greatest damping due to the interaction with fluid mud. An idealized 1-D model helped to explain the observations.

1. Introduction

Field observation of wave–mud interaction has been long conducted in many muddy coastal areas over the world. The wave damping over the mudbanks of the Mississippi Delta was first quantified in the field by Tubman and Suhayda (1977). The authors observed that the energy loss resulting from the wave–mud interaction was at least one order of magnitude higher than that related to frictional effects that are typical from sandy environments. Wells and Kemp (1986) calculated the wave energy loss along a transect off the mud coast of Suriname. The authors reported that more than 90% of the spectral energy of the waves was damped out as they propagated over the muddy path from 8 to 1.5 m depth. More recently, the field observations by Mathew et al. (1995) showed that 75–80% of wave energy is attenuated as the waves travel 1.1 km over the mudbank off Kerala coast, India. Field measurements in the Persian Gulf presented in the work by Haghshenas and Soltanpour (2011) revealed that the wave energy is attenuated by 25 to 90% depending significantly on the period of incoming waves. The authors concluded that the maximum dissipation of the wave energy due to the presence of fluid mud occurred in the frequency band around 0.16 Hz (6 s) throughout the measurement period. In this paper, two distinct datasets are analyzed aiming at providing better insights on the wave damping phenomena at the Brazilian coast.

Extensive mud deposits are observed off Cassino Beach, Southern Brazil. According to Vinzon et al. (2008) this deposit mainly originates from the fine sediments flushed from the adjacent Patos Lagoon (Fig. 1) especially when northerly winds are persistent. This condition favors the deposit formation that is mostly located between 6 and 15 m depth.

During storms, the energetic incoming waves occasionally transport the mud deposit to the foreshore. In these situations, the typical sandy beach is covered with a substantial amount of mud. This is a unique process along the Brazilian coastline that jeopardizes recreation and endangers the fauna (Calliari et al., 2000; Pereira et al., 2011).

The extension of the mud deposit was determined by sediment sampling and combined acoustic methods such as single (210 Hz) and dual (33 – 200 kHz) frequency echo-sounding and also high-resolution seismic surveying (2 – 16 KHz) (Calliari et al., 2000, 2008; Dias and Alves, 2008). The observations showed that the onshore limit of the mud bank presents a relatively sharp transition between sand and mud, at depths varying from 3 to 6 m depth and the offshore limit is located about 17 m depth, from where the sand content gradually increases seaward. The grain size distribution of bottom sediment samples showed 75% to 100% of mud (silt + clay), with the clay size fraction comprising 25% to 59% of the sample. The clay fraction is mostly composed of smectite (40%) and illite (34%). The high content of smectite confers high cohesiveness to the material expressed by its high cation exchange capacity which ranged between 74.3 to 169.2 meq/100 g. Samples collected at depths deeper than 20 m, were classified as fine to very fine sands with D50 varying from 0.1 mm to 0.138 mm. Such samples contain from 3% to 21% of mud with a maximum of 6.2% of clay size particles.

The action of water waves over a soft marine mud bottom can rework the mud layer, elevating this interface to a height that depends on the balance between both mechanical energy imparted to raise the potential energy of the suspension and the negative buoyancy of the suspension beneath the interface (Vinzon and Mehta, 1998). In a feedback way, this mud layer plays an important role in the wave damping

* Corresponding author.
E-mail address: s.meirellesnunesdarocha@tudelft.nl (S. Meirelles).
[1] Previously: Department of Coastal & Oceanographic Engineering, Federal University of Rio de Janeiro.

http://dx.doi.org/10.1016/j.margeo.2016.03.006
0025-3227/© 2015 Published by Elsevier B.V.

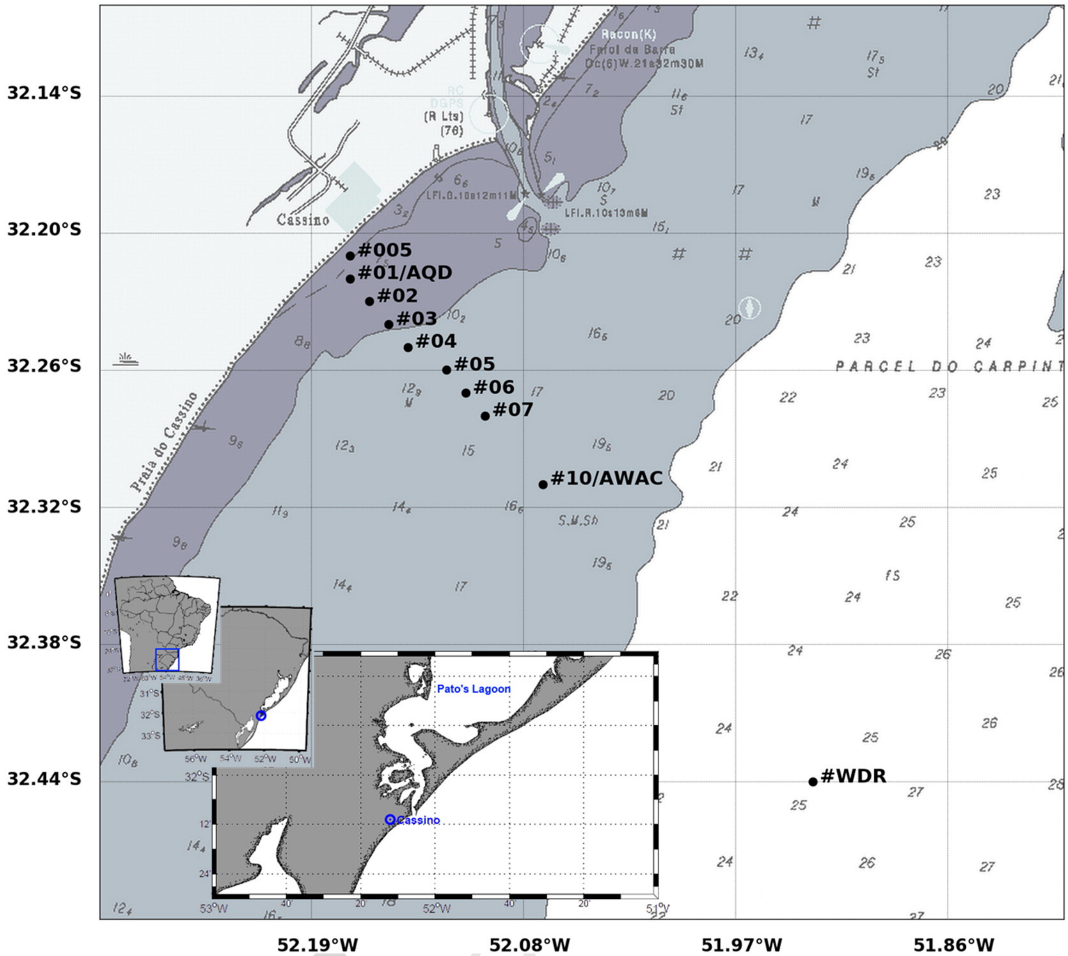

Fig. 1. Cassino Beach location and the measurement stations along a shore-perpendicular transect. During the 2005 campaign, a Waverider (WDR) was deployed at 25 m depth along with an Aquadopp (AQD) placed at 8 m. In 2008, an AWAC was deployed permanently at 18 m depth (#10) while the other instruments measured successively on the stations numbered from #07 to #005 along a transect towards the shore (see text for details).

by viscous dissipation (Darlrymple and Liu, 1978; Torres-Freyermuth and Hsu, 2010). The theoretical background of the wave attenuation due to fluid mud has been described under a number of frameworks but in all cases the damping rate varies as a function of the mud layer thickness, viscosity, density and the water depth (Gade, 1958; De Wit, 1995; Ng, 2000; Kranenburg et al., 2011).

Aiming to investigate the dynamic behavior of the mud deposit under wave action, a series of field experiments called Cassino Project, started in 2004. In Holland et al. (2009) the main aspects of the data collection of this project are summarized. Initially, the characteristics of the deposit were determined by using geo-acoustic methods and in situ sampling for laboratory analysis enabling to identify the extension, thickness and relevant aspects of the mud deposit. Wave measurement devices were deployed in a transect along the main direction of the incident waves so as to register the attenuation induced by the mud deposit. Rogers and Holland (2008) thoroughly analyzed the wave data collected in 2005 using different mud-wave damping modeling approaches. The authors showed that the extension, thickness, density and viscosity of the mud deposit are critical parameters for simulating the wave attenuation observed through the mud deposit. The deposit characteristics remained constant during the simulated time series as there was no sufficient information about its spatial and temporal variability. As a result, more detailed observations were recommended in order to fine-tune the validation of the dissipation mechanisms. The lack of information about the bed characteristics and its relation with the wave damping motivated a new set of experiments which were carried out in 2008.

The new measuring strategy considered the transient properties of the mud deposit as a function of the local wave regime. Therefore, data collection of the wave parameters and the mud characteristics was conducted concomitantly. Furthermore, the dataset of 2005 was further inspected so that the wave spectra were divided in four predetermined frequency bands that are representative of the wave climate (see Section 3 for details). The advantage of this technique is that it allowed the assessment of the wave energy dissipation for distinct sea states that are represented by each of the frequency bands.

2. Field work

In the fall 2005, wave measurements took place simultaneously at two locations. One offshore location, situated at 25 m depth, where a Waverider Datawell© (WRD) was deployed providing information about the undisturbed waves entering the system and a second location near the landward border of the mud patch at 7−8 m depth where an Aquadopp Nortek© (AQD) was installed (Fig. 1).

In 2008, simultaneous data collection of the wave field and the vertical structure of the mud layer was conducted (Fig. 1). The measurements covered the same transect of the 2005 measurements however with more cross-shore resolution such that the locations were approximately 1.5 km apart from each other. Wave parameters were measured continuously at 18 m depth with an AWAC Nortek©. At successive stations moving towards the coast waves were obtained with an ADV Nortek© at same time that density profiles were determined with a DensiTune Stema Sytem©. This density measuring probe is based on

Please cite this article as: Meirelles, S., Vinzon, S.B., Field observation of wave damping by fluid mud, Marine Geology (2015), http://dx.doi.org/10.1016/j.margeo.2016.03.006

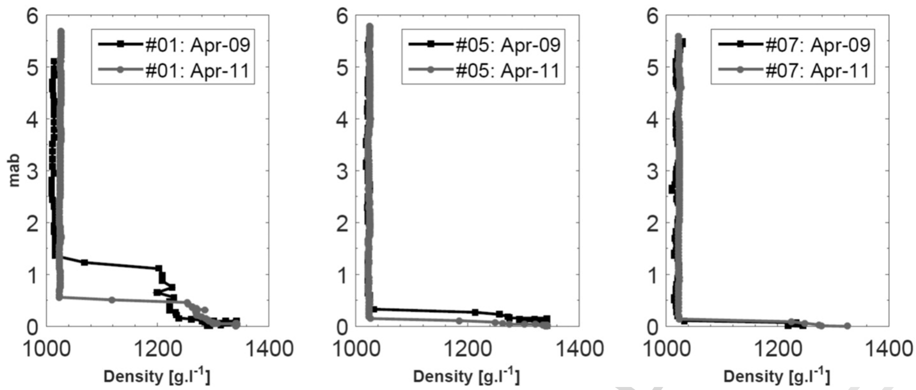

Fig. 2. Variation of the lutocline height in the stations #01, #05 and #07 from April 9th (black line) to 11th (gray line).

the response of a vibrating-fork, provided with a pressure sensor. The probe was launched from the boat at each station, recording the density profile. In addition, bottom samples and sediment cores were collected in order to calibrate and to validate the DensiTune results.

The risks of losing instruments in the muddy environment together with the intense local fishing activities limited the realization of measurements to a relatively short period. In order to circumvent this problem, all field operations were carried out from a boat. The downside was that the data collection occurred only during calm weather conditions.

3. Methodology

3.1. Waverider

The Waverider acquired data for about 42.5 days. At every full hour the wave buoy recorded for 1800 s at 1.28 Hz. The directional spectra were obtained from the surface displacement series through conventional cross-spectral analysis between the vertical and horizontal components of the displacement.

Before computing the directional spectra, every record was divided in 32 segments with 64 points which gives 64 degrees of freedom (dof). In this way the statistical properties of the samples are preserved within the recorded time (ergodic process) and consequently the variant characteristics of the series (noises) were minimized or even eliminated (Parente, 2001).

Frequencies lower than 0.05 and higher than 0.30 Hz were discarded. In general, the coherence function between the vertical and horizontal components of displacement presented relatively low values outside the mentioned frequency interval.

3.2. Aquadopp/AWAC/ADV

The Aquadopp measurements covered the same period of 42.5 days of the Waverider. The instrument sampled at 2 Hz comprising 2048 samples per record. The wave spectra were computed via the PUV technique (see Bishop and Donelan, 1987) in which the pressure and the horizontal components of velocity are scaled up using a transfer function. Thus, the near the bottom spectra are translated into surface-wave spectra.

An undesirable limitation lies in the attenuation of the pressure signal with the increasing depth. This leads to unrealistic values when the transfer function is applied causing an exponential growth of the higher frequencies of the spectra. The coherence function reflected this behavior therefore the values outside the interval between 0.05 and 0.3 Hz were discarded.

The PUV technique was also applied to the AWAC and ADV dataset. The AWAC, deployed at station #10, was setup to measure ≈34 min of wave parameters every hour with sampling rate of 1 Hz. The ADV recorded 4098 samples at 2 Hz in the shallower stations of the transect.

3.3. Density profile

At least three DensiTune casts were carried out at every location in which the profile with less interference was chosen. The advantage of the probe is that it gives real-time information allowing the user to immediately detect the quality of a given profile. Ideally, this instrument needs to be lowered at approximately 1 m/s. The boat motion was a potential source of noise in the data therefore the boat was anchored to be lined up with the incoming waves. The instrument was validated against direct sediment density measurement from sub-samples taken from sediment cores that were collected in stations #01, #03 and #05. The correlation between both methods varied from 65 to 95%.

The profiles were smoothed through a moving average. The distance between the pressure sensor and the vibrating-fork is automatically corrected with the instrument software. In this study only the downcasts were considered in the analysis.

The fluid mud was defined here as the density values within the interval from 1080 to 1250 $g \cdot l^{-1}$. The consolidated bed was considered as the maximum depth that the DensiTune could penetrate into the deposit that was nearly the same for all the stations. This enabled to compare the vertical variability of the deposit over time as exemplified in Fig. 2. Within 2 days the lutocline height lowered about 0.80 *m* with an associated increase of the density at station #01.

3.4. The DAAT

The Directional Analysis with Adaptive Techniques (DAAT) is meant to detect the occurrence of different sea states in a wave record based on wavelet analysis (Parente, 2001). This technique was originally applied to determine the multi-directional character of a sea-state even when two directional components present the same frequency. The directional aspect of the DAAT comes with a cost: the resolution in frequency is sacrificed so as to increase resolution in the directional domain (more details in Parente, 2001). A trade-off between frequency and directional resolution is needed to avoid this limitation. Thus the frequency domain is adequately divided in frequency bands that are well representative of the wave climate.

The DAAT was applied to the Waverider and Aquadopp records. In the present study, the advantage of the DAAT owns to the capacity to

Table 1
Frequency bands used in the DAAT. Q1

Band number	Frequency interval (period)
1	0.05 to 0.09 Hz (18.7 to 11.3 s)
2	0.09 to 0.12 Hz (11.3 to 8.05 s)
3	0.12 to 0.16 Hz (8.05 to 6.25 s)
4	0.16 to 0.26 Hz (6.25 to 3.75 s)

Please cite this article as: Meirelles, S., Vinzon, S.B., Field observation of wave damping by fluid mud, Marine Geology (2015), http://dx.doi.org/10.1016/j.margeo.2016.03.006

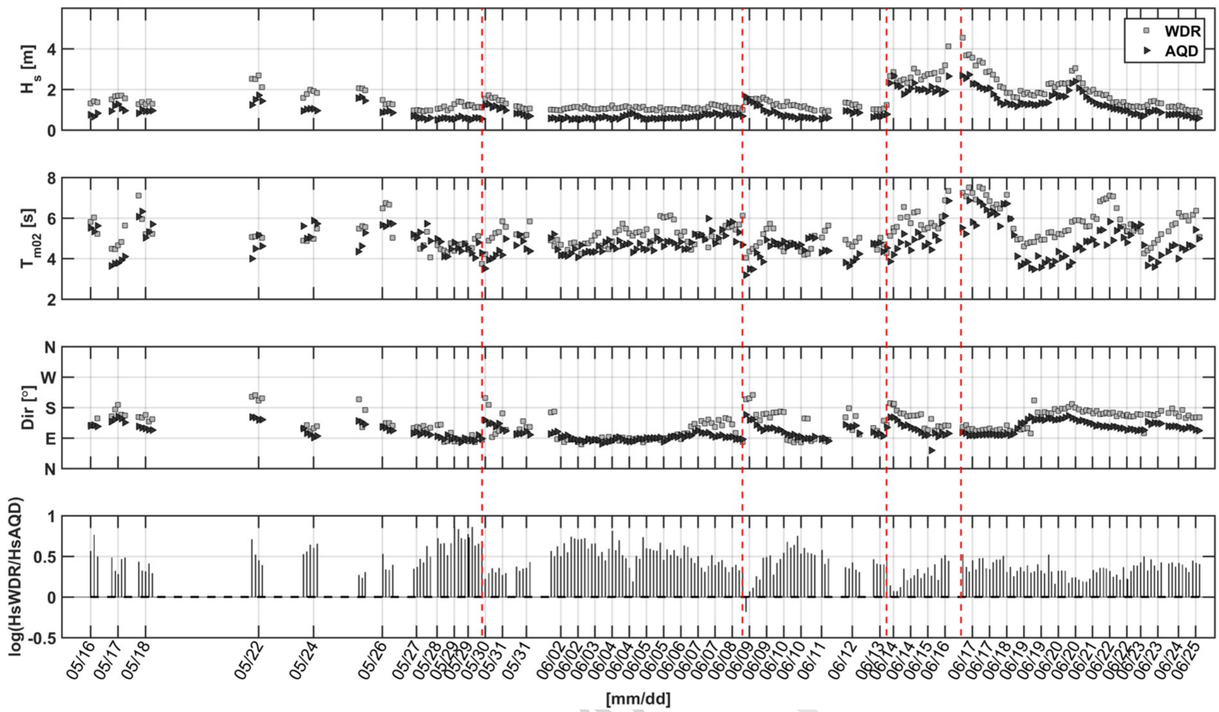

Fig. 3. Waverider (WDR) and Aquadopp (AQD) series from the 2005 observations. From top to bottom: [1] significant wave height; [2] wave mean period; [3] wave direction; and [4] dissipation ratio based on the wave height decay that is given by log(*HsWDR*/*HsAQD*). The gaps in the series are due to error in the Waverider measurement or to desynchronization between the Waverider and the Aquadopp measurements. The vertical dashed line depict the storm events discussed in the text.

assess the wave energy dissipation for distinct sea states that are representative of the local wave climate. In other words, the wave damping is investigated for different wind-sea and swell events. The selected frequency bands are shown in Table 1. It is important to stress out that the lengths of the wave series measured in 2008 were too short to apply the DAAT technique.

4. Observed wave damping

As previously explained, the dataset of the 2005 campaign was re-analyzed in order to get new insights on the wave energy decay along the shore-normal transect. According to the 2005 measurements by (Holland et al., 2009) the thickness of the mudbank was on the order

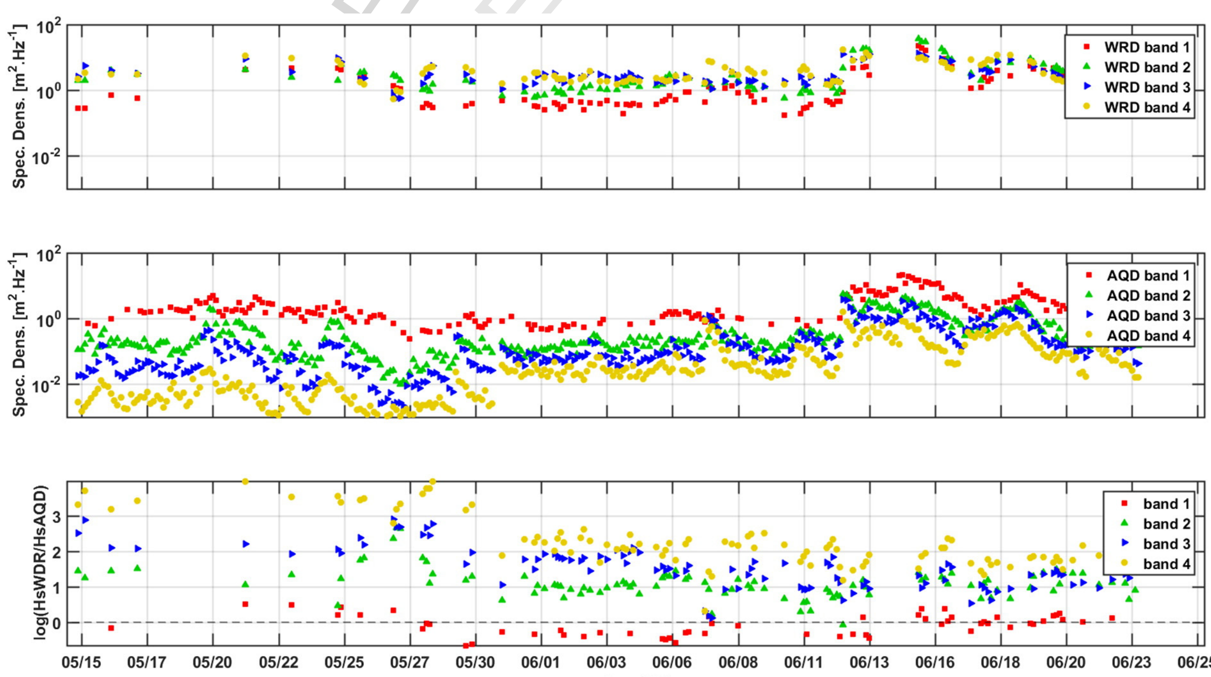

Fig. 4. The first two panels show the temporal evolution of each frequency band determined by the DAAT technique (band 1 — red marks; band 2 — green marks; band 3 — blue marks; band 4 — yellow marks; WDR — Waverider; AQD — Aquadopp). The bottom panel depicts the series of the dissipation ratio for each frequency band. Note that the band 1 (red marks) exhibits some negative values indicating that energy was transfered from higher to lower frequencies. (For interpretation of the references to color in this figure legend, the reader is referred to the web version of this article.)

Please cite this article as: Meirelles, S., Vinzon, S.B., Field observation of wave damping by fluid mud, Marine Geology (2015), http://dx.doi.org/10.1016/j.margeo.2016.03.006

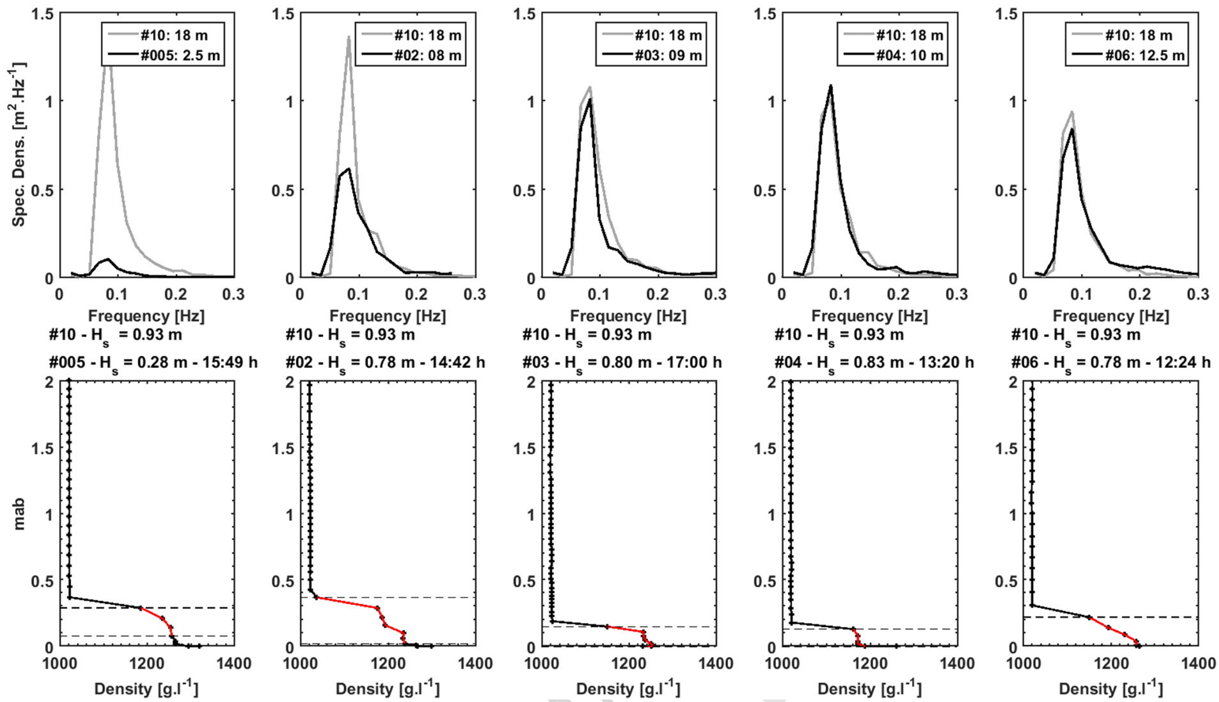

Fig. 5. Wave attenuation towards the shore. Upper panels: Wave spectra of the foremost station #10 (gray line) compared to the wave spectra of the shallower stations #08, #04, #03, #02 and #005 (black line). Lower panels: corresponding density profiles of the shallower stations (mab — meters above the bed). The red line indicates the fluid mud limits considered in the present work ($1080 < \rho_{mud} \leq 1250\ g \cdot l^{-1}$).

of 0.40 m with densities around 1140 g · l and typical viscosity of 0.0076 $m^2 \cdot s^{-1}$. Fig. 3 presents the wave parameters measured at 25 and 8 m depth. In general, the offshore station recorded higher waves with slightly higher mean period in comparison with the nearshore station. The incoming waves were mainly from SE and the changes in direction from deep to shallower waters were minor suggesting that the effects of refraction are likely to take place in even deeper water. The dissipation ratio, given by log(HsWDR/HsAQD), was computed from the 1D spectra of the Waverider and Aquadopp series. In general, the decay of energy did not present a clear pattern with respect to changes in the significant wave height. This behavior is expected to be a result of feedback mechanism between the wave action and the deposit characteristics.

The results also show that the higher dissipation values are associated with fair weather conditions. After the storm passages (see vertical dashed lines in Fig. 3) the dissipation decreased abruptly and gradually the attenuation rate rose again in the subsequent waning period. Similar aspect was also found by Haghshenas and Soltanpour (2011) in the Persian Gulf where the observed dissipation rates ranged from 64 to 90% during events of calm sea condition whereas the maximum dissipation rate during storm was about 50%.

Calliari et al. (2000) attributed the migration of the fluid mud to those more energetic events that occurs at Cassino Beach. The high waves are responsible for the fluidization of the more compacted mud, re-suspending the bed material and transporting it shorewards. This partially explains the behavior of the dissipation ratio with respect to the wave action but, for example, there was no sudden decreasing of the attenuation when the strongest storm recorded past by. The wave damping is also depending on the wave frequency, as demonstrated, for example, by Torres-Freyermuth and Hsu (2010) and Sheremet et al. (2011). Such dependency can elucidate the differences seen in the dissipation ratio shown by Fig. 3. In this regard, the DAAT technique served as a tool to investigate how wind-sea and swell are affected by the mud deposit.

Fig. 4 reveals that bands 3 and 4 contain more energy throughout the Waverider record except in the period of the strongest storm when the lower frequency bands gained more energy. The evolution of the spectrum bands towards the shore exhibited a different pattern. The Aquadopp series showed a successively energy decay from band 1 to band 4. This demonstrates that bands 3 and 4 underwent significant energy loss implying that wind-sea are more susceptible to be affected by the fluid mud than swells.

The dissipation ratio was also calculated for each of the frequency bands (Fig. 4). This analysis confirms that the highest attenuation ratios are seen in frequency bands 3 and 4 over the entire series. At the lower frequencies (swells), there was limited dissipation specially for waves longer than ≈11 s (band 1). This spectral band has even gained energy at some periods while dissipation increased for higher frequencies. This evidence suggests that non-linear wave transfer takes place towards lower frequencies independently on the sea state and the fluid mud (Elgar and Raubenheimer, 2008). On the other hand, the viscous dissipation prevails at higher frequencies.

The DAAT provided evidences of the potential higher attenuation of the waves generated by the local wind. Mild storms (mixed sea states) are likely to disturb the deposit (and vice-versa) more effectively. The incidence of long swells seems to not be significantly affected by the mud. The uncertainties regarding the mud rheology and distribution of the 2005 dataset prevent more conclusive inferences about the role of viscous dissipation in damping the waves. Rogers and Holland (2008) indirectly inferred the mud properties at Cassino Beach 2005 experiment via inverse modeling using the measured surface attenuation. Although this approach served to give first insights on the mud thickness and distribution, it is not accurate because it assumes constant viscosity. Hsu et al. (2013) demonstrated that the viscosity response to the

Table 2
Settings used in the 1-D model to build the JONSWAP spectra.

Model run	Mud layer height [m]	Hs [m]	Dir [°]	Tp [s]
MUD0	Up to 1	0.9	0	12
MUD20	Up to 1	0.9	20	12
NOMUD	0	0.9	0	12

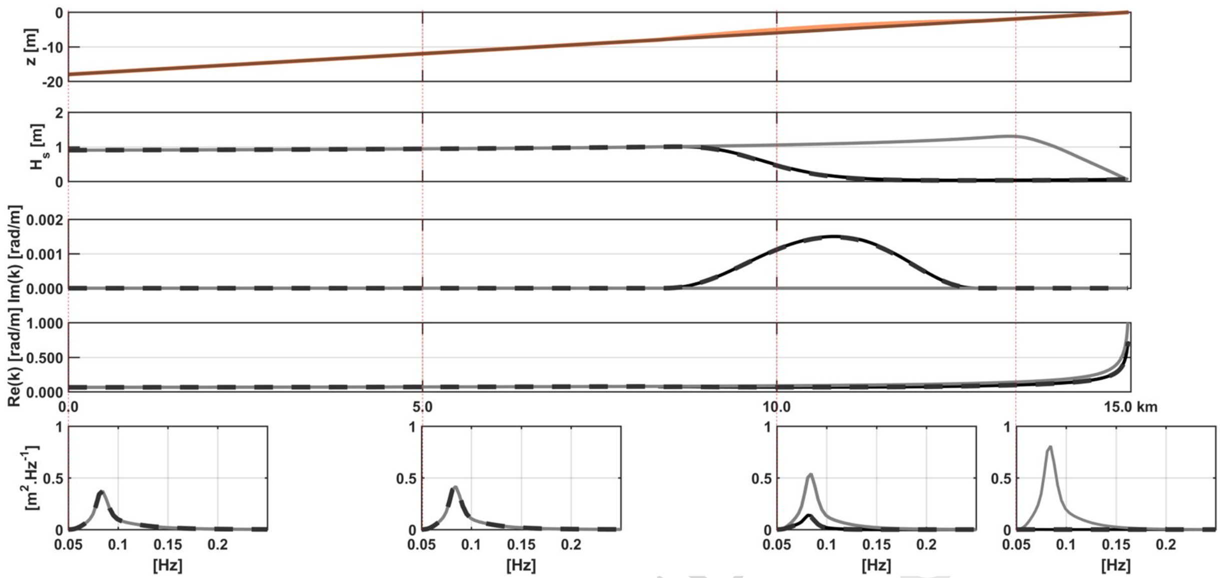

Fig. 6. Model results for the idealized cases: MUD0 (black line), MUD20 (dashed black line) and NOMUD (gray line). From top to bottom: [1] bottom profile (dark brown) and mud layer (light brown); [2] significant wave height; [3] viscous dissipation given by the imaginary part of the wave number; [3] bottom friction given by the real part of the wave number; and [4] 1-D normalized spectra of three idealized runs in four different locations: 0, 5, 10 and 13.5 km from the offshore boundary.

wave action is highly phase-dependent and non-Newtonian, especially for less energetic conditions. Therefore the observations of 2008 focused more on the variability of the deposit.

The 2008 measurements showed that the characteristics of the vertical structure of the deposit played a important role on the wave energy damping. An increasing thickness of the fluid mud layer was observed moving from offshore to onshore. Fig. 5 shows the wave spectra recorded at the foremost station #10 compared to the shallower stations and their corresponding density profiles.

This dataset was obtained on April 10. From locations #06 to #03, the typical shallow water wave transformation are possibly prevailing over the viscous dissipation as seen by the increasing energy in the vicinities of the peak frequency of the spectra that suggests shoaling effects. As the wave travels towards the depocenter, the fluid mud become more important and about 90.7% of the spectral energy is dissipated. The wave damping increased dramatically in a quite short distance, from station #02 to #005, where the mud layer thickness also increased significantly.

The maximum damping is believed to have occurred in the center of the deposit (station #01) characterized by the most thick mud layer along the transect. At this location the lutocline height reached almost 1.5 m which was enough to attenuate the whole spectrum range.

To get more clear insights on the effects of the viscous dissipation on the wave spectra, an idealized scenario representing the average conditions found on April 10, 2008 was simulated with a 1-D spectral model (Kranenburg et al., 2011). Three simulations were analyzed regarding the behavior of the spectral evolution for: [1] the effects of the fluid mud layer (with density and viscosity equal to 1250 $g \cdot l{-}1$ and 0.5 $m^2 \cdot s^{-1}$, respectively) on the shore-perpendicular incoming waves (run MUD0); [2] the effect of refraction (run MUD20); and [3] the effects of bottom friction alone (run NOMUD) (Table 2).

The results illustrated the distinction between the effects of viscous dissipation and bottom friction (Fig. 6). When the mud layer is disregarded (NOMUD), the computation showed that the wave height grows monotonically up to the breaking point as a result of the shoaling. This effect is responsible for the augment of the peak energy of the wave spectra as they travel towards the shore (Fig. 6). The simulations also indicated that the effects of bottom friction, given by the real part of the wave number, are more pronounced near the break and in the surfzone.

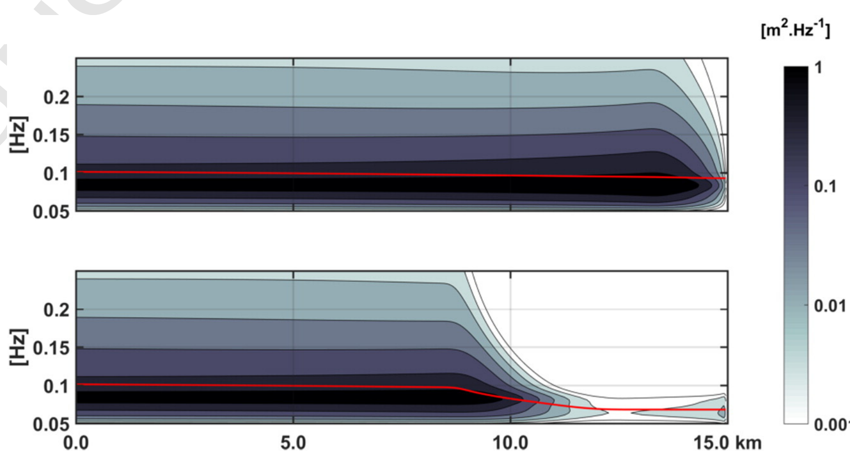

Fig. 7. Spectral evolution towards shallow waters for cases NOMUD (top panel) and MUD0. The red line depicts the mean frequency.

Please cite this article as: Meirelles, S., Vinzon, S.B., Field observation of wave damping by fluid mud, Marine Geology (2015), http://dx.doi.org/10.1016/j.margeo.2016.03.006

When the mud layer is activated in the model (MUD0), the spectral energy is dramatically dissipated as soon as the waves enter the mudbank and they are fully attenuated after passing over the depocenter (Fig. 6). The simulations presented qualitatively a good agreement with the measurements on April 10 suggesting that the viscous dissipation is the dominant process on attenuating the wave height. The imaginary wave number, that represents the dissipation rate, increased proportionally to the mud layer thickness so that the dissipation reached its maximum at the depocenter. The effects of refraction (MUD20) appeared to be meaningless as the simulations showed almost identical behavior as in MUD0. Non-linear interactions were not considered because the model presented unrealistic values as also reported byKranenburg et al. (2011).

Regarding the dissipation over the spectrum bandwidth, Fig. 7 portrays the spectral evolution for the cases MUD0 and NOMUD. According to the simulations, it seemed that the bottom friction effects act more evenly throughout the spectral frequencies whereas the viscous dissipation, given the deposit characteristics, is more effective at higher frequencies. As a consequence there is a sharp shift of the mean frequency towards lower frequencies when the waves travel over the mudbank. These simulations corroborate the findings of the DAAT technique.

5. Concluding remarks

The present study showed that the wave energy dissipation over muddy bottom is more effective during fair weather conditions, when wind-sea waves are predominant. The observed decrease of lutocline height was associated to the development of a swell. This evidence indicates that low frequency waves may be less effective in disturbing the mud deposit. The reduction of damping observed during mild storms and the increasing dissipation ratios when wind-sea are dominant are in agreement with other field observations (Traykovski et al., 2015). Swell waves generated during severe storms are less affected by viscous dissipation however it is expected to be an important transport mechanism of the fluid mud.

The observed larger damping of shorter waves is in qualitative agreement with the existing theories (e.g., Gade, 1958; Kranenburg, 2008). Yet, the field observations by (Haghshenas and Soltanpour, 2011) found a persistent stronger dissipation around the wave period of 6 s which would be equivalent of band 4 in the present study. Despite the similarities concerning the dissipation of a preferential frequency band, the motives for that are not straightforward. For example, the sea states found at the Cassino Beach are quite different than those at the Persian Gulf such that the response of the fluid mud to the wave action will affect differently the rheological properties of the deposit and hence it would lead to differentiations in the viscous dissipation over the wave spectrum.

The lower frequencies showed no or little dissipation, or even gaining energy in some periods of the time series. This phenomenon cannot be explained by traditional two layer models (Kranenburg et al., 2011). Torres-Freyermuth and Hsu (2014) found that the viscosity can dictate whether infragravity waves are attenuated or not. Neither viscosity effects nor infragravity waves were taken into account in the analysis presented in this study. Therefore it is still unclear how wave groupiness and its associated bound long wave interact with the mud viscosity on the Cassino Beach.

Large spatio-temporal variability of the bed properties is of crucial importance regarding the viscous dissipation. The effective damp occurred in the vicinities of the depocenter, where the lutocline height increased significantly in a short distance. The interplay between the dynamics of the deposit and short waves is not yet clear therefore more research is necessary with respect to the damping of the different frequency components of the wave spectrum.

Measurements during calm weather, despite being limited, showed to be useful so that the spatio-temporal variability of the mud deposit could be mapped out. The DensiTune may also help to get in situ information of mud viscosity after proper calibration that was not available during the 2008 field work.

Simultaneous measurements of wave and bed properties along the wave propagation path are required to improve our understanding on wave damping and to validate existing models. If calibrated, a model can bring valuable information of the prevalence of viscous dissipation over bottom friction.

It is worth noting that the Cassino Beach undergoes seasonal variabilities concerning the typical morpho- and hydrodynamic regimes. This denotes that the dataset presented here may not be representative of all conditions found offshore Cassino Beach. Finally, this dataset can be made available upon request.

Acknowledgments

This work was made possible through grants by the Office of Naval Research (N00173-05-1-G26, N00173-04-1-G901 and N00014-04-1-0274) administered through the ONR International Field Office, CNPq for the scholarship granted to the authors. We acknowledge Fabio Nacimento, Tiago Leao and the team from LOG/FURG, in particular Prof. Lauro Calliari, for their valuable collaboration. The authors are indebted to Prof. Parente for his assistance with the wave analysis and for providing the DAAT code.

References

Bishop, C.T., Donelan, M.A., 1987. Measuring waves with pressure transducer. Coast. Eng. 11, 309–328.
Calliari, L.J., Speranski, N.S., Torronteguy, M., Oliveira, M.B., 2000. The mud banks of cassino beach, southern Brazil: characteristics, processes and effects. J. Coast. Res. 1–9 (ICS 2000 Proceedings).
Calliari, L.J., Winterwerp, J.C., Fernandes, E., Cuchiara, D., Vinzon, S.B., Sperle, M., Holland, K.T., 2008. Fine grain sediment transport and deposition in the Patos Lagoon–Cassino Beach sedimentary system. Cont. Shelf Res. 15 http://dx.doi.org/10.1016/j.csr.2008.09.019.
Darlrymple, R.A., Liu, P.L.-F., 1978. Waves over soft muds: a two-layer fluid model. J. Phys. Oceanogr. 8, 1121–1131.
De Wit, P.J., 1995. Liquefaction of Cohesive Sediments Caused by Waves Ph.D. thesis Delft University of Technology (194 pp.).
Dias, C.R.R., Alves, M.L., 2008. Geotechnical properties of Cassino Beach mud. Cont. Shelf Res. 4 http://dx.doi.org/10.1016/j.csr.2008.09.015.
Elgar, S., Raubenheimer, B., 2008. Wave dissipation by muddy seafloors. Geophys. Res. Lett. 35, 1–5.
Gade, H.G., 1958. Effects of a nonrigid, impermeable bottom on plane surface waves in shallow water. J. Mar. Res. 16, 61–85.
Haghshenas, S.A., Soltanpour, M., 2011. An analysis of wave dissipation at the hendijan mud coast, the Persian Gulf. Ocean Dyn. 61, 217–232.
Holland, K.T., Vinzon, S.B., iari, L.J., 2009. A field study of coastal dynamics on muddy coast offshore of Cassino Beach, Brazil. Cont. Shelf Res. 29, 503–514.
Hsu, W.Y., Hwung, H.H., Hsu, T.J., Torres-Freyermuth, A., Yang, R.Y., 2013. An experimental and numerical investigation on wave-mud interactions. J. Geophys. Res. Oceans 118, 1126–1141. http://dx.doi.org/10.1002/jgrc.20103.
Kranenburg, W., 2008. Modelling Wave Damping by Fluid Mud. Master's thesis Delft University of Technology (152 pp.).
Kranenburg, W., Winterwerp, J., de Boer, G., Cornelisse, J., Zijlema, M., 2011. Swan-mud: engineering model for mud-induced wave damping. J. Hydraul. Eng. 137, 959–975.
Mathew, J., Baba, M., Kurian, N., 1995a. Mudbanks of the southwest coast of india. I: wave characteristics. J. Coast. Res. 168–178.
Ng, C.-O., 2000. Water waves over a muddy bed: a two-layer stokes' boundary layer model. Coast. Eng. 40, 221–242.
Parente, C.E., 2001. DAAT — a new technique for wave directional analysis. Ocean Wave Measurement and Analysis (2001) (chapter 28).
Pereira, P., Calliari, L., Holman, R., Holland, K., Guedes, R., Amorin, C., Cavalcanti, P., 2011. Video and field observations of wave attenuation in a muddy surf zone. Mar. Geol. 279, 210–221. http://dx.doi.org/10.1016/j.margeo.2010.11.004 (URL: http://www.sciencedirect.com/science/article/pii/S0025322710003099).
Rogers, W.E., Holland, K.T., 2008. A study of dissipation of wind-waves by mud at Cassino Beach, Brazil: prediction and inversion. Cont. Shelf Res.
Sheremet, A., Jaramillo, S., Su, S.-F., Allison, M.A., Holland, K.T., 2011. Wave-mud interaction over the muddy atchafalaya subaqueous clinoform, Louisiana, United States: wave processes. J. Geophys. Res. Oceans 116, C06005. http://dx.doi.org/10.1029/2010JC006644 (n/a–n/a).
Torres-Freyermuth, A., Hsu, T.-J., 2010. On the dynamics of wave–mud interaction: a numerical study. J. Geophys. Res. Oceans 115, C07014. http://dx.doi.org/10.1029/2009JC005552 (n/a–n/a).
Torres-Freyermuth, A., Hsu, T.-J., 2014. On the mechanisms of low-frequency wave attenuation by muddy seabeds. Geophys. Res. Lett. 41, 2870–2875. http://dx.doi.org/10.1002/2014GL060008.

Traykovski, P., Trowbridge, J., Kineke, G., 2015. Mechanisms of surface wave energy dissipation over a high-concentration sediment suspension. J. Geophys. Res. Oceans 120, 1638–1681. http://dx.doi.org/10.1002/2014JC010245.

Tubman, M.W., Suhayda, J.N., 1977. Wave action and bottom movements in fine sediments. Technical Report DTIC Document.

Vinzon, S.B., Mehta, A., 1998. A mechanism for the formation of lutoclines by waves. J. Waterw. Port Coast. Ocean Eng. 124, 147–149.

Vinzon, S.B., Winterwerp, J.C., Nogueira, R., de Boer, G.J., 2008. Mud deposit formation on the open coast of the larger patos lagoon's cassino beach system. Cont. Shelf Res. 17 http://dx.doi.org/10.1016/j.csr.2008.09.021.

Wells, J.T., Kemp, G.P., 1986. Interaction of surface waves and cohesive sediments: field observations and geologic significance. Estuarine Cohesive Sediment Dynamics. Springer, pp. 43–65.

Please cite this article as: Meirelles, S., Vinzon, S.B., Field observation of wave damping by fluid mud, Marine Geology (2015), http://dx.doi.org/10.1016/j.margeo.2016.03.006